Journal of Neurochemistry

JOURNAL OF NEUROCHEMISTRY | 2010 | 114 | 488–498 doi: 10.1111/j.1471-4159.2010.06781.x

Neuroprotection against superoxide anion radical by metallocorroles in cellular and murine models of optic neuropathy

Akiyasu Kanamori,* Maria-Magdalena Catrinescu,* Atif Mahammed,† Zeev Gross† and Leonard A. Levin*,‡

*Maisonneuve-Rosemont Hospital Research Center and Department of Ophthalmology, University of Montreal, Montreal, Quebec, Canada

†Schulich Faculty of Chemistry, Technion – Israel Institute of Technology, Haifa, Israel

‡Department of Ophthalmology and Visual Sciences, University of Wisconsin School of Medicine and Public Health, Wisconsin, USA

Abstract

Corroles are tetrapyrrolic macrocycles that have come under increased attention because of their unique capabilities for oxidation catalysis, reduction catalysis, and biomedical applications. Corrole-metal complexes (metallocorroles) can decompose certain reactive oxygen species (ROS), similar to metalloporphyrins. We investigated whether Fe-, Mn-, and Ga-corroles have neuroprotective effects on neurons and correlated this with superoxide scavenging activity *in vitro* and *in vivo*. Apoptosis was induced in retinal ganglion cell-5 neuronal precursor cells by serum deprivation. Cell death was measured with sodium 3′-[1-[(phenylamino)-carbonyl]-3,4-tetrazolium]-bis (4-methoxy-6-nitro) benzene-sulfonic acid hydrate and calcein-AM/propidium iodide assays. Fe- and Mn-corroles, but not the non-redox-active Ga-corrole used as control, reduced RGC-5 cell death after serum deprivation. Serum deprivation caused increased levels of intracellular superoxide, detected by an increase in the fluorescence intensity of 2-hydroxyethidium, and this was blocked by Fe- and Mn-corroles, but not Ga-corrole. *In vivo* real-time confocal imaging of retinas after optic nerve transection assessed the superoxide production within individual rat retinal ganglion cells. Fe- and Mn-corroles, but not Ga-corrole, scavenged neuronal superoxide *in vivo*. Given that the neuroprotective activity of metallocorroles correlated with superoxide scavenging activity, Fe- and Mn-corroles could be candidate drugs for delaying neuronal death after axonal injury in optic neuropathies, such as glaucoma.

Keywords: metallocorroles, neuroprotection, neurons, superoxide, optic neuropathy.

J. Neurochem. (2010) **114**, 488–498.

Superoxide, the result of the one electron reduction of dioxygen, can serve as an intracellular signaling molecule for a variety of biologically processes. It also reacts with nitric oxide (NO) as to form peroxynitrite (HOONO), a toxin involved in numerous diseases (Pacher *et al.* 2007). We previously showed that generation of superoxide is a critical molecular event underlying neuronal death induced by axonal injury (Lieven *et al.* 2003, 2006; Nguyen *et al.* 2003) and *in vivo* imaging demonstrates that superoxide elevation precedes apoptosis in axotomized neurons (Kanamori *et al.* in press). Intracellular delivery of pegylated superoxide dismutase-1 (SOD), which dismutates superoxide into H_2O_2, inhibits neuronal death after axotomy *in vitro* (Schlieve *et al.* 2006) and *in vivo* (Kanamori *et al.* in press), presumably by interfering with a superoxide signal for apoptosis. This mechanism has therapeutic implications for disease associated with axonal injury.

However, translation of a therapy that relies on intracellular protein delivery is less practical than one that utilizes small molecules. We therefore took advantage of

Received February 12, 2010; revised manuscript received April 15, 2010; Accepted April 19, 2010.

Address correspondence and reprint requests to Leonard A. Levin, M.D., Ph.D., Maisonneuve-Rosemont Hospital, 5415 boul. de l'Assomption, Montréal, Quebec, Canada H1T 2M4 or Zeev Gross, Ph.D., Schulich Faculty of Chemistry, Technion City, Technion, Haifa 32,000, Israel. E-mail: lalevin@facstaff.wisc.edu or chr10zg@tx.technion.ac.il

Abbreviations used: 2-OH-Et, 2-hydroxyethidium; BSA, bovine serum albumin; CSLO, confocal scanning laser ophthalmoscopy; DiR, 1,1′-dioctadecyl-3,3,3′,3′-tetramethylindotricarbocyanine iodide; HEt, hydroethidine; HOONO, peroxynitrite; NO, nitric oxide; PI, propidium iodide; RGC, retinal ganglion cell; ROS, reactive oxygen species; SOD, superoxide dismutase; XTT, sodium 3′-[1-[(phenylamino)-carbonyl]-3,4-tetrazolium]-bis (4-methoxy-6-nitro) benzene-sulfonic acid hydrate.

Table 1 Reactive oxygen species scavenging by metallocorroles

	Superoxide dismutase activity, $k_{cat}/M^{-1}s^{-1}$		Decomposition of peroxynitrite, $k_{cat}/M^{-1}s^{-1}$	Catalase activity, $k_{cat}/M^{-1}s^{-1}$
	Cytochrome *c* assay	Pulse radiolysis	Stopped-flow	Stopped-flow
$Fe(tpfc)(SO_3H)_2$	1.7×10^6 (a)	3×10^6 (a)	3.1×10^6 (c)	4.3×10^3 (d)
$Mn(tpfc)(SO_3H)_2$	4.8×10^5 (a)	$< 1 \times 10^5$ (a)	8.6×10^4 (c)	ND
Mn(TMPyP)	3.8×10^6 (b)	5.6×10^6 (a)	Not catalytic (data in the presence of ascorbate co-reductant: 3.3×10^4) (e)	20 (f)
$Ga(tpfc)(SO_3H)_2$	Inactive (d)	Inactive (d)	Inactive (d)	Inactive (d)

a, Data from Eckshtain *et al.* (2009); b, data from Batinic-Haberle *et al.* (1998); c, data from Mahammed and Gross (2006); d, A. Mahammed and Z. Gross, unpublished data; e, data from Crow (1999); f, data from Day *et al.* (1997).

recent developments in metallocorrole chemistry as a means of using small molecules to modulate superoxide signaling. Corroles are tetrapyrrolic macrocycles with a porphyrin-like inner core containing four nitrogen atoms serving as an equatorial coordination template for metal ions. Depending on the metal, these molecules can function as components in oxidation catalysis (Fe, Mn, Cr), reduction catalysis (Cr, Mn, Fe), group transfer catalysis (Rh, Fe), sensors of gaseous molecules (Co), and medicinal research (Aviv and Gross 2007; Aviv-Harel and Gross 2009). The latter includes research performed on cellular and murine models of cancer (Agadjanian *et al.* 2006; Agadjanian *et al.* 2009), cardiovascular (Haber *et al.* 2008), diabetes (Okun *et al.* 2009), and neurodegenerative diseases (Kupershmidt *et al.* 2010). Over the past decade they have received increasing attention, following the major discoveries for their facile synthesis (Gross and Galili 1999; Gryko 2002). Porphyrins have been used in numerous applications, including the use of metalloporphyrins as neuroprotective agents that work via decomposition of ROS (Cuzzocrea *et al.* 2001). We predicted that metallocorroles, some of which can be highly specific ROS scavengers (reviewed in Table 1), might be useful small molecule drugs for inhibiting ROS-mediated signaling of cell death.

To study this, we investigated the neuroprotective effect of iron (Fe), manganese (Mn), and gallium (Ga) corroles (Fig. 1) in both *in vitro* and *in vivo* models of neuronal death. For the *in vitro* studies, we used serum-deprived neuronal precursor retinal ganglion cell (RGC)-5 cells, which when differentiated with low levels of staurosporine, have several features similar to that of mature neurons (Frassetto *et al.* 2006). For *in vivo* studies, we used confocal scanning laser ophthalmoscopy (CSLO) coupled with intravitreal fluorescent dyes to demonstrate that certain metallocorroles function as SOD mimetics.

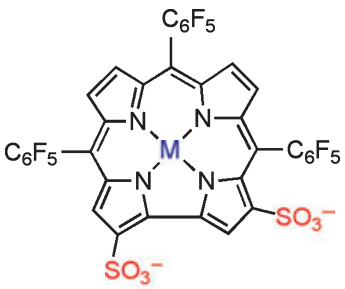

Fig. 1 Chemical structure of metallocorroles used in the study.

Methods

Materials

RGC-5 cells were a generous gift of Neeraj Agarwal, Ph.D.; Dulbecco's modified Eagle's medium and fetal bovine serum were from GIBCO (Grand Island, NY, USA) Staurosporine was from Alexis Biochemicals (San Diego, CA, USA). Menadione, penicillin-streptomycin and sodium 3′-[1-[(phenylamino)-carbonyl]-3,4-tetrazolium]-bis (4-methoxy-6- nitro) benzene-sulfonic acid hydrate (XTT) were from Sigma-Aldrich (St. Louis, MO, USA). Calcein-AM, propidium iodide (PI), 1,1′-dioctadecyl-3,3,3′,3′-tetramethylindotricarbocyanine iodide [DiR; DiIC18(7)], and hydroethidine (HEt) were from Invitrogen (Eugene, OR, USA).

Metallocorrole synthesis

The iron(III), manganese(III), and gallium(III) complexes of 2,17-bis-sulfonato-5,10,15-tris(pentafluorophenyl)corrole (Fe(tpfc)$(SO_3H)_2$, Mn(tpfc)$(SO_3H)_2$, Ga(tpfc)$(SO_3H)_2$) were synthesized as described previously (Saltsman *et al.* 2002; Mahammed and Gross 2005).

Mn(tpfc)(SO$_3$H)$_2$

A flask loaded with a 10 mL of N,N-dimethylformamide solution of 2,17-bis-sulfonato-5,10,15-tris(pentafluorophenyl)corrole (H_3(tpfc)(SO_3H)$_2$, 15 mg, 16 μmol), and Mn(OAc)$_2$•4H$_2$O (15 mg, 61 μmol) was heated to reflux for 15 min, followed by evaporation of the solvent. The inorganic salts were separated by column chromatography on silica (eluent: ethanol), affording 15 mg (15 μmol, 94% yield) of the manganese(III) complex of H_3(tpfc)(SO_3H)$_2$. ^{19}F NMR (CD_3OD): δ = −123.0 (brs, *ortho*-F), −128.0 (brs, *ortho*-F), −131.0 (brs, *ortho*-F), −153.5 (s, *para*-F), −154.1 (s, *para*-F), −156.6 (s, *para*-F), −159.5 (s, *meta*-F), −162.9 (s, *meta*-F). UV/vis (buffer solution, pH 7.30) λ_{max} [ε(M^{-1} cm^{-1})] = 392 (19 000), 422 (21 000), 480 (17 000), 644 (11 500), 610 (9500), 576 (9000). MS (matrix-assisted laser desorption/ionization-time of flight mass spectrometry): *m/z* 1007.9 [M^+, 100%], 1008.9 [MH^+, 85%].

Ga(tpfc)(SO$_3$H)$_2$

A solution of H_3(tpfc)(SO_3H)$_2$ (20 mg, 21 μmol) in pyridine (10 mL) was added to a flask that contains a large excess (about 0.2 g) of flame-dried $GaCl_3$, and the reaction mixture was heated to reflux for 30 min under argon, followed by evaporation of the solvent. The product was dissolved in 75 mL basic water (0.1 M Na_2CO_3) and washed with three portions of dichloromethane. The water was evaporated and the inorganic salts were separated by column chromatography on silica (eluent, ethanol), affording 19 mg (19 μmol, 90% yield) of the gallium(III) complex of H_3(tpfc)(SO_3H)$_2$. ^{1}H NMR (CD_3OD): δ = 9.89 (s, 1H), 8.84 (s, 1H), 8.78 [d, ^3J(H,H)] 4.8 Hz, 1H), 8.65 (d, ^3J(H,H) = 4.8 Hz, 1H), 8.55 (t, ^3J(H,H) = 4.3 Hz, 2H). ^{19}F NMR (CD_3OD): δ = −139.0 (d, ^3J(F,F) = 23.0 Hz, 2F, *ortho*-F), −140.4 (d, ^3J(F,F) = 23.5 Hz, 4F, *ortho*-F), −157.6 (t, ^3J(F,F) = 20.1 Hz, 1F, *para*-F), −158.2 (t, ^3J(F,F) = 20.5 Hz, 1F, *para*-F), −160.2 (t, ^3J(F,F) = 20.3 Hz, 1F, *para*-F), −166.3 (m, 4F, *meta*-F), −169.1 (m, 2F, *meta*-F). UV/vis (buffer solution, pH 7.30) λ_{max} [ε(M^{-1} cm^{-1})] = 424 (75 000), 588 (13 600), 610 (17 300). MS (matrix-assisted laser desorption/ionization-time of flight mass spectrometry): *m/z* 1022.2 [M^+, 100%] and a characteristic isotopic pattern of 1023.2 (55%), 1024.2 (92%), 1025.2 (58%). MS (electrospray): *m/z* 509.9 [(M − 2H)/2]$^-$.

Fe(tpfc)(SO$_3$H)$_2$

One portion of FeCl$_2$•4H$_2$O (55 mg, 277 mmol) was added at once to a pyridine solution (20 mL) of H_3(tpfc)(SO_3H)$_2$ (240 mg, 251 μmol), and the mixture was heated immediately to reflux for 5 min under argon, followed by evaporation of the solvent. The inorganic salts were separated by column chromatography on silica (eluent: ethanol), affording 240 mg (238 μmol, 95% yield) of the iron(III) complex of H_3(tpfc)(SO_3H)$_2$. ^{19}F NMR (CD_3OD): δ = −106.2 (brs, *ortho*-F), −115.4 (brs, *ortho*-F), −116.5 (brs, *ortho*-F), −149.8 (s, *para*-F), −150.5 (s, *para*-F), −154.5 (s, *para*-F), −156.2 (s, *meta*-F), −157.2 (s, *meta*-F), −160.2 (s, *meta*-F). UV-vis (buffer solution, pH 7.00) λ_{max} [ε(M^{-1} cm^{-1})] = 404 (34 000), 552 (12 000), 738 (2300). MS (electrospray): *m/z* 503.5 [(M − 2H)/2]$^-$.

Cell culture

RGC-5 cells were cultured in Dulbecco's modified Eagle's medium containing 1 g/L glucose, 10% fetal bovine serum, 100 U/mL penicillin, and 100 μg/mL streptomycin. Cells were split every 48–72 h when cells were approximately 60–75% confluent, replated at a 1 : 20 dilution in a 25 cm^2 flask in 5 mL of cell culture media and incubated at 37°C in humidified 5% CO_2.

Treatments

RGC-5 cells were seeded onto 6-well or 96-well microplates and pre-incubated for 24 h. Differentiation was induced with staurosporine (316 nM) for 4 h. RGC-5 cells were then serum deprived for 48 h in the presence or absence of metallocorroles.

Assessment of cell viability

XTT assay

XTT assays were used to determine the effects of treatment on cell viability. XTT, a tetrazolium salt, is cleaved by dehydrogenation in metabolically active cells, yielding a highly colored, water-soluble formazan product. In non-dividing cells, where there is no proliferation, the XTT signal is essentially proportional to the number of viable cells. Unlike other tetrazolium salts, such as (3-(4,5-dimethylthiazol-2-yl)-2,5-diphenyltetrazolium bromide, XTT does not require solubilization of formazan crystal prior to absorbance measurements. The XTT labeling and electron coupling reagents were added to treated serum-deprived or non-deprived cells 4 h before spectrophotometric analysis. All XTT assays were performed in 96-well microplates. Optical density was measured on a microplate reader (BioTek ELx808, Winooski, VT, USA) with a 490-nm test wavelength and a 630-nm reference wavelength. Negative controls (no cells) and positive controls (cells without serum deprivation) were assayed in parallel. $N = 8$ per condition. Experiments were performed in triplicate.

Fluorescent live-dead assays

RGC-5 cells were seeded onto coverslips in six-well microplates. After treatment with metallocorroles or vehicle for 48 h in serum deprivation, media was aspirated from wells and cells stained with 1 μM calcein-AM and 4 μM PI in phosphate-buffered saline (PBS) for 30 min. The staining solution was aspirated and replaced with PBS. Cells were fixed with 4% paraformaldehyde and coverslips mounted on slide glasses using PermaFluor (Thermo Scientific, Walthan, MA, USa). Slides were photographed under epifluorescence and digitized. Three visual fields were randomly sampled from each well, at least 50 cells were counted from each field, and three wells were analyzed for each condition. Live (calcein-positive) and dead (PI-positive) cells were manually counted by an observer masked to the treatment group.

Measurement of intracellular superoxide

Cells were assessed for the production of superoxide by visualizing the reaction of HEt with superoxide, which forms 2-hydroxyethidium (2-OH-Et). HEt is a non-fluorescent, reduced form of ethidium that can passively cross plasma membranes of live cells. When HEt is oxidized to 2-OH-Et by superoxide, it can bind to DNA and yield fluorescence in the red spectrum (excitation 480 nm/emission 567 nm) (Zhao *et al.* 2003). Assays were performed in six-well microplates in triplicate. After 48 h of serum deprivation in the presence or absence of metallocorrole, HEt (50 μM) was added to the medium of cells 30 min before the end of the serum deprivation period to visualize superoxide.

Incubation of cells with menadione (1 mM) for 30 min was used as a positive control for production of superoxide. After incubation of HEt, cells were washed with PBS and digitally captured by quantitative epifluorescence microscopy. Three wells were tested for each group and three microscope fields were randomly sampled from each well at the same exposure setting. The excitation spectra of 2-OH-Et and other HEt oxidation products are similar at medium wavelengths (540–580 nm), but differ at short wavelengths (370–400 nm), allowing the use of different excitation filters in *ex vivo* fluorescence microscopy to distinguish the two species (Robinson *et al.* 2006). Cells that fluoresce when excited at 395 nm are 2-OH-Et-positive, while cells fluorescing when excited at 560 nm are positive for all HEt oxidation products. We therefore used two filter sets for HEt fluorescent microscopy. A 395 ± 5.5 nm excitation, 500 nm dichroic, and 562 ± 20 nm emission filter was used to selectively image 2-OH-Et, and a 560 ± 20 nm excitation, 595 nm dichroic, and 630 ± 30 nm emission was used to non-selectively image all HEt oxidation products. ImageJ (National Institutes of Health, Bethesda, MD, USA) was used to quantify the HEt signals. Briefly, cells in captured fields were segmented by Set Threshold From Background. Mean fluorescence intensity and granularity (standard deviation of all pixel intensities) of single cells were then evaluated by Analyze Particle.

Measurement of superoxide *in vivo*

To test the effect of metallocorroles on superoxide *in vivo*, the optic nerve was intraorbitally transected in Long-Evans rats as described (Kanamori *et al.* 2010) and levels of superoxide studied by intravitreal injection of HEt followed by *in vivo* CSLO. To confirm the localization of the product of superoxide with HEt, RGCs were retrogradely labeled by stereotactically injecting 2.1 μL of DiR (20 mg/mL) into each superior colliculus of rats 5 days before optic nerve transection (Kanamori *et al.* in press). Axotomy by optic nerve transection causes apoptosis of RGCs. HEt or corrole + HEt was injected into the vitreous 3 days after transection. The vitreous concentration of HEt and corrole were 100 μM and 100 nM, respectively, based on a vitreous volume in the rat of 56 μM (Berkowitz *et al.* 1998). The next day, retinal imaging by CSLO was performed under ketamine/xylazine anesthesia. Pupils were dilated with phenylephrine/atropine. Retinal images were obtained using a 30° field of view and real-time averaging of at least 50 images on a Heidelberg Retina Angiograph II (Heidelberg Engineering, Germany) CSLO at 93% sensitivity. The plane of focus was adjusted to the inner retina by imaging the nerve fiber layer at 488 nm.

Statistics

Viability was assessed as percentage of control, and compared with untreated controls within each experiment. Means were compared using Student's unpaired *t*-test. All data are shown as mean ± SEM. Significant difference required $p < 0.05$.

Results

Metallocorrole toxicity

Given that the toxicity of metallocorroles on RGC-5 cells was unknown, we tested a wide range of concentrations (10 nM–100 μM) of metallocorroles in cultures of the RGC-5 neuronal precursor cell line in the presence of serum for 48 h. Fe-, Mn-, and Ga-corroles had no effect on viability of undifferentiated and differentiated RGC-5 cells at concentrations of ≤ 1 μM (Fig. 2). Cell death ranged from 13% to 40% with 10 μM concentrations of all metallocorroles in the presence of serum. The toxicity of the metallocorroles at 10 μM was significantly greater in the absence of serum, which induced 37–80% cell death (Fig. 2b).

The greater toxicity of metallocorroles when serum was absent made it difficult to determine their capacity for preventing or delaying neuronal death in a serum deprivation model. We therefore tested several serum and serum-free conditions to find a functional paradigm for serum deprivation without significant metallocorrole toxicity. Bovine serum albumin (BSA) at a concentration of 10 mg/mL did not affect RGC-5 survival rates in the presence of 1% serum, while it dramatically decreased the toxicity of metallocorroles in the absence of serum. For example, the survival rate of undifferentiated cells with 10 μM Fe-corrole was increased from 29 ± 1.7% to 63 ± 4.4% ($p < 0.001$) in the presence of 1% BSA (Fig. 2b).

Metallocorroles prevent neuronal cell death from serum deprivation

Two different approaches were taken to evaluate the neuroprotective effects of metallocorroles. First, to compare the protective efficacy of different metallocorroles, undifferentiated or differentiated RGC-5 cells were exposed to serum deprivation with and without 1% BSA for 48 h in the presence of varying concentrations (1 nM–10 μM) of each metallocorrole. Cell viability was determined by XTT assay. Serum deprivation significantly reduced the viability of RGC-5 cells to approximately 60% of control. Addition of Fe- and Mn-corroles rescued these cells in a dose-dependent fashion with an optimal concentration range of 10–100 nM in the absence of serum (Fig. 3). Ga-corrole was not neuroprotective at any concentration in RGC-5 cells. The neuroprotective effects of Fe- and Mn-corroles were greater in the presence of 1% BSA (Fig. 3), presumably by decreasing metallocorrole toxicity that was exacerbated by the absence of protein.

To demonstrate that these results were not confounded by the method used to determine viability, i.e. the chemical reduction of XTT, a redox-independent viability assay was also used, i.e. calcein-AM/PI (live/dead) double staining. In undifferentiated RGC-5 cells, there were very few PI-positive cells in control cultures (Fig. 4). Serum deprivation significantly increased the proportion of PI-positive cells from 1.0 ± 0.3% to 5.2 ± 0.1% ($p < 0.005$). Addition of Fe-corrole at concentrations of 10 nM or 100 nM to serum-deprived cells significantly decreased the proportion of PI-positive cells (10 nM: 2.3 ± 1.1%, $p = 0.03$ vs. control; 100 nM: 1.7 ±

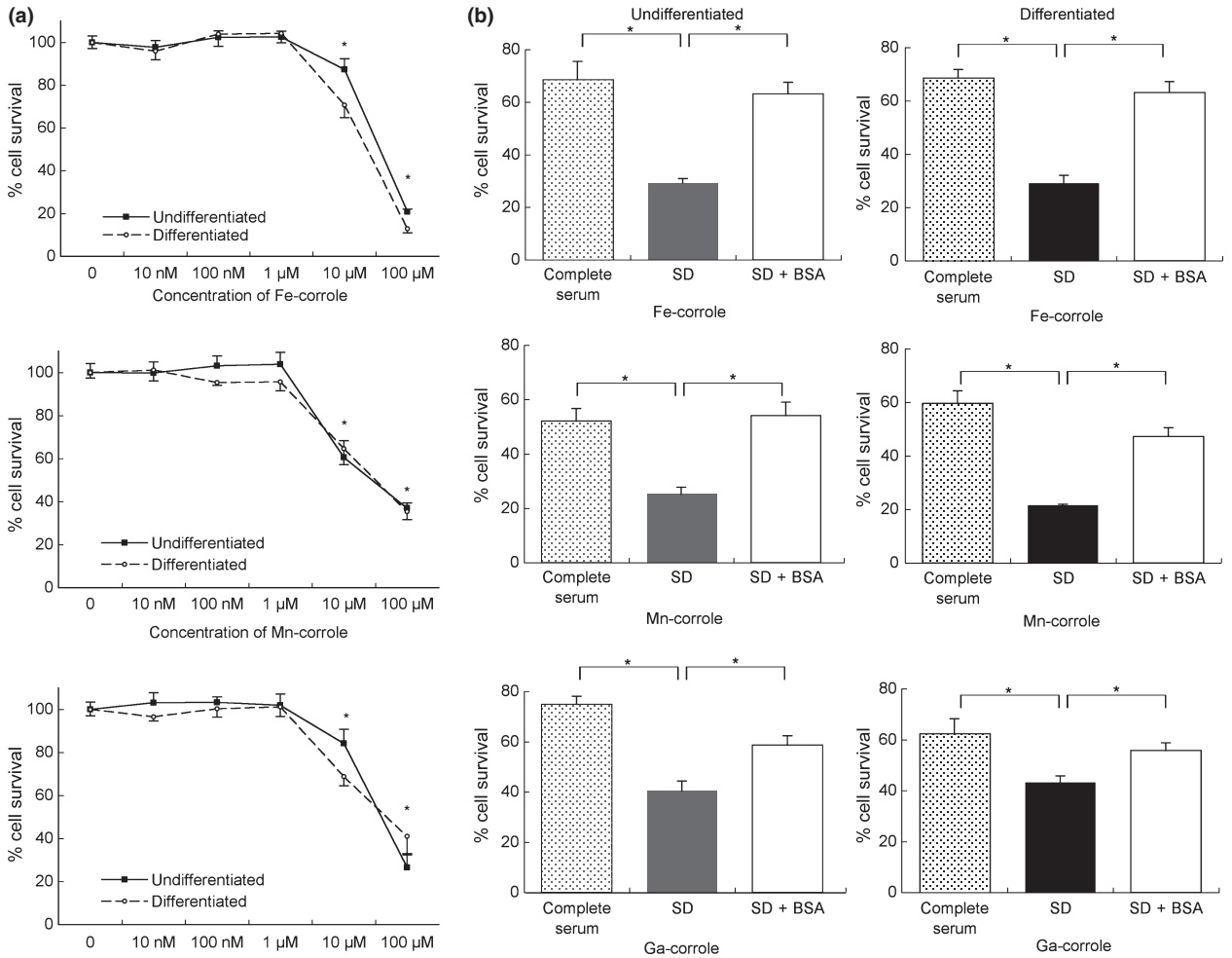

Fig. 2 Metallocorroles are toxic only at high concentrations. (a) Undifferentiated and differentiated retinal ganglion cell (RGC)-5 cells in complete media (10% serum) were treated with increasing concentrations of Fe, Mn, and Ga-corroles. Cell survival was measured by sodium 3′-[1-[(phenylamino)-carbonyl]-3,4-tetrazolium]-bis (4-methoxy-6- nitro) benzene-sulfonic acid hydrate assay. *$p < 0.05$ between the samples treated with and without metallocorroles. (b) RGC-5 cells were treated with or without a high (10 μM) concentration of Fe, Mn, and Ga-corroles in complete (10% serum) media (stippled bars), serum-deprived media (closed bars) and serum-deprived media containing 1% bovine serum albumin (BSA) (open bars). BSA decreased the toxicity of metallocorroles in the absence of serum. SD, serum deprivation, *$p < 0.05$.

0.2%, $p = 0.002$ vs. control). Similarly, Mn-corrole at concentrations of 10 nM or 100 nM decreased PI-positivity (10 nM: 1.3 ± 0.1%, $p < 0.001$ vs. control; 100 nM: 1.5 ± 0.5%, $p = 0.002$ vs. control) (Fig. 4b). On the other hand, there was no significant difference in PI-positivity in serum-deprived cells treated with and without Ga-corrole, indicating an absence of neuroprotection. All metallocorroles at 10 μM increased the number of PI-positive cells, indicating toxicity at that concentration.

In RGC-5 cells differentiated with staurosporine, the proportion of PI-positive cells in normal conditions was 6.6 ± 0.8%, suggesting a baseline level of apoptosis from the treatment. This increased with serum deprivation to 35 ± 2.1%. Fe and Mn-corroles but not Ga-corrole decreased the proportion of PI-positive cells at concentrations of 10 and 100 nM [Fe (10 nM): 16 ± 5.6%, $p = 0.03$; Fe (100 nM): 18 ± 1.2%, $p = 0.002$; Mn (10 nM): 32 ± 1.5%, $p = 0.031$; Mn (100 nM): 31 ± 2.9%, $p = 0.041$).

Serum deprivation induces superoxide production

Intracellular superoxide was visualized by imaging fluorescence of 2-OH-Et, the product of HEt and superoxide (Fig. 5). Excitation filters that were selective (395 nm) or non-selective (560 nm) for 2-OH-Et were used to generate epifluorescent images of serum-deprived cells. The fluorescence intensity seen with 2-OH-Et-selective excitation was less than with the non-selective excitation because the bandwidth of the former filter was much narrower than the

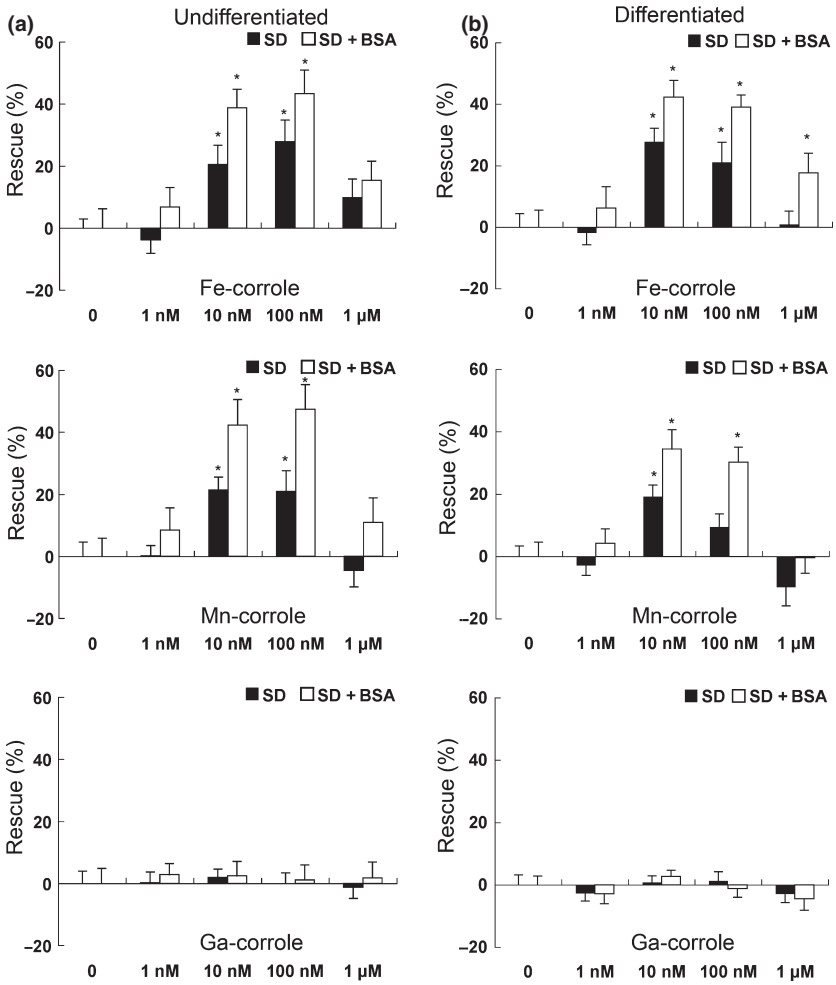

Fig. 3 Undifferentiated (left) or differentiated (right) retinal ganglion cell (RGC)-5 cells serum-deprived in 1% bovine serum albumin (BSA) were treated with increasing concentrations of Fe-, Mn-, or Ga-corroles. The rescue from serum deprivation was measured by sodium 3′-[1-[(phenylamino)-carbonyl]-3,4-tetrazolium]-bis (4-methoxy-6-nitro) benzene-sulfonic acid hydrate assay, normalized to 100% rescue with serum. Closed and open bars show serum deprivation (SD) and SD with 1% BSA, respectively. $^*p < 0.05$ between the samples treated with and without metallocorroles in SD. These data are summarized from three independent experiments.

latter (11 vs. 40 nm). The mean intensity per cell was used to measure total amount of superoxide, and granularity (standard deviation of all pixels within a cell) of intensity used to indicate dispersion of superoxide from subcellular compartments. Dying cells with shrinkage of cell body had high granularity. In both undifferentiated and differentiated RGC-5 cells, serum deprivation increased the fluorescence intensity and granularity, compared with serum-containing controls. Fe- and Mn-corroles (100 nM) significantly suppressed the increase of superoxide in undifferentiated and differentiated RGC-5 cells. Ga-corrole (100 nM) did not have a significant effect on superoxide levels. Menadione (1 mM), used as a positive control for superoxide induction, resulted in a burst of 2-OH-Et in both undifferentiated and differentiated RGC-5 cells. To prove that superoxide and not another ROS was being imaged, cells were incubated with polyethylene glycol-conjugated superoxide dismutase, which crosses cell membranes and dismutates superoxide into hydrogen peroxide. Polyethylene glycol-conjugated superoxide dismutase (30 U/mL) reduced 2-OH-Et levels in serum-deprived differentiated cells from 133.2 ± 5.7 to 75.1 ± 4.4 arbitrary light units ($p < 0.001$).

Metallocorroles scavenge axotomy-induced superoxide *in vivo*

In vivo detection of superoxide in RGCs after axotomy was carried out by CSLO after intravitreal injection of HEt. Two built-in CSLO lasers were utilized. The 488 nm laser was used for excitation of 2-OH-Et and the 788 nm laser was used for excitation of DiR. Cells positive for 2-OH-Et after optic nerve transection could be localized to the ganglion cell layer by confocal focusing on the innermost retina, and identified as being in RGCs by colocalization with the retrogradely transported fluorescent dye DiR (Fig. 6a–c). CSLO images of eight retinal quadrants immediately adjacent to the optic nerve head were obtained at each session, and positive cells counted (Fig. 6e). Optic nerve transection increased the number of 2-OH-Et-positive cells (Fig. 6f). Fluorescence was absent in the outer retina and retinas with untransected optic nerves. The peak of 2-OH-Et positivity was seen at 4 days after axotomy (66.2 ± 11.6 cells/retina). Therefore, we counted the number of 2-OH-Et-positive cells at 4 days after transection in retinas treated with ($n = 4$) and without metallocorrroles ($n = 8$). Fe- and Mn-corroles (100 nM), but not Ga-corrole, significantly decreased the

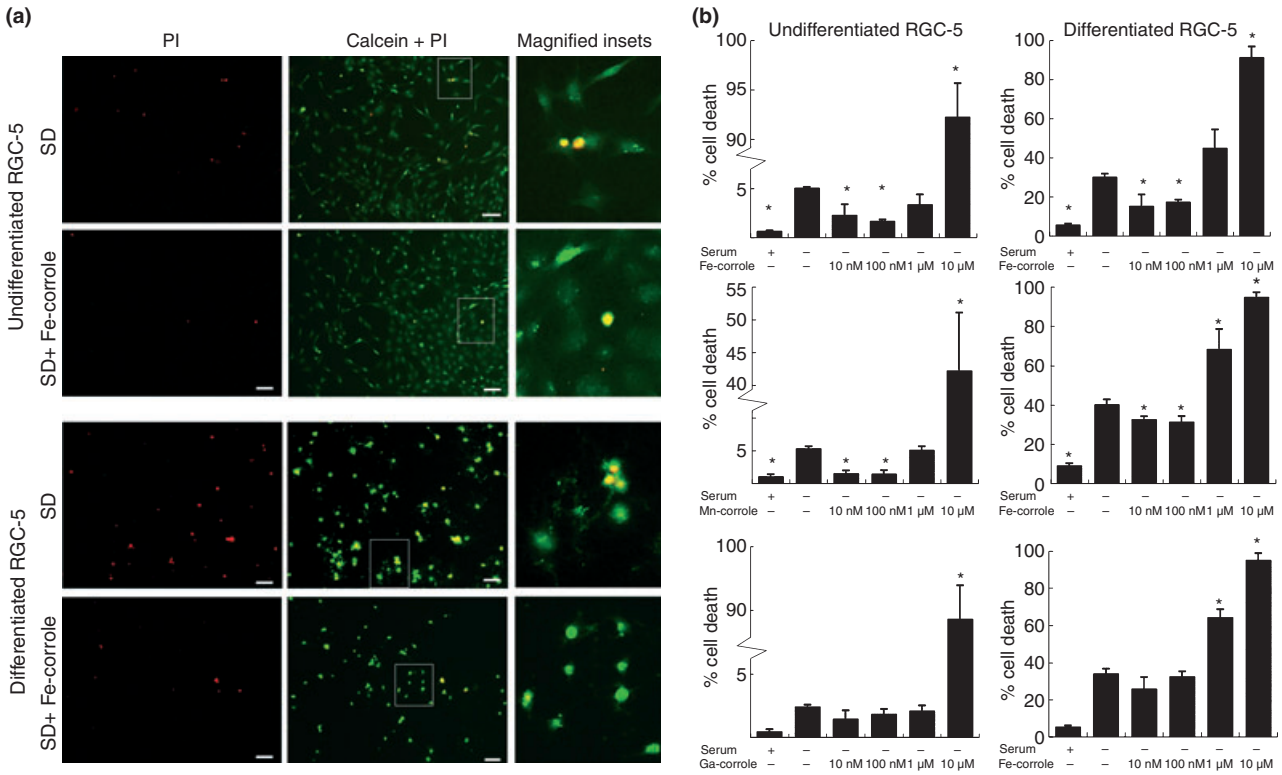

Fig. 4 (a) Representative photomicrographs of retinal ganglion cell (RGC)-5 cells stained with calcein-AM/propidium iodide (PI). Undifferentiated or differentiated RGC-5 cells were treated with either serum deprivation without metallocorroles or serum deprivation with 100 nM Fe-corrole. (Left) Propidium iodide (red) staining of dead cells. (Center) Merge of propidium iodide and calcein (green). Green staining indicates live cells and yellow indicates late apoptotic/necrotic cells. (Right) Magnified insets from outlined fields in center column. Scale bar, 20 μm. SD, serum deprivation. (b) Summary of calcein-AM/PI cell-survival assay data. Quantitative data from fluorescence images derived from the calcein/PI cell-survival assay are expressed as the mean ± SEM of results from three wells in each condition. Three microscope fields containing more than 50 cells were randomly sampled from each well. *$p < 0.05$ compared with serum-deprived RGC-5 without metallocorroles.

number of superoxide-positive cells/retina (Fe: 20 ± 11.0, $p = 0.028$; Mn: 22.5 ± 6.8, $p = 0.013$; Ga: 49.5 ± 5.9, $p = 0.26$), as shown in Fig. 6f.

Discussion

These results demonstrate that (i) Fe- and Mn-corroles but not Ga-corrole significantly reduce cell death induced by serum deprivation in neuronal precursor cells; (ii) Fe- and Mn-corroles but not Ga-corrole significantly decrease superoxide levels in tissue culture; (iii) Fe- and Mn-corroles significantly decrease superoxide levels in RGCs after axotomy *in vivo*. Together, these findings suggest that not only are metallocorroles a novel class of neuroprotectants, but that the mechanism of action covaries with a reduction in intracellular superoxide levels *in vitro* and *in vivo*.

Studies in purely chemical systems demonstrate that metallocorroles are powerful ROS scavengers (Table 1). Fe-corrole is a potent SOD mimetic, with similar activity to the extensively studied (Mn(III)tetrakis(1-methyl-4-pyridyl)porphyrin pentachloride, Mn-corrole has slightly lower levels of SOD activity, and Ga-corrole is inactive (Eckshtain *et al.* 2009). Fe- and Mn-corrole shorten the half-life of HOONO, the product of superoxide and NO, very significantly (Fe > Mn), and Ga-corrole is inactive (Mahammed and Gross 2006). Fe-corrole but not Ga-corrole catalyzes the decomposition of H_2O_2. These and other ROS are critical for specific types of neuronal death. Superoxide is necessary for the signaling of apoptosis after axonal injury (Lieven *et al.* 2003; Kanamori *et al.* in press), while HOONO is a potent initiator of neuronal cell death and is linked to several neurodegenerative disorders (Torreilles *et al.* 1999).

Some metalloporphyrins, particularly Fe- and Mn-porphyrins, mimic SOD and decompose superoxide and HOONO quite efficiently. Neuroprotective effects of Mn-porphyrins as SOD mimetics have been demonstrated in animal models of ischemia (Salvemini *et al.* 1999; Mackensen *et al.* 2001; Sheng *et al.* 2002). Fe-porphyrins acting as HOONO decomposition catalysts protect cytokine-induced cytotoxicity in hippocampal cultures (Misko *et al.* 1998) and

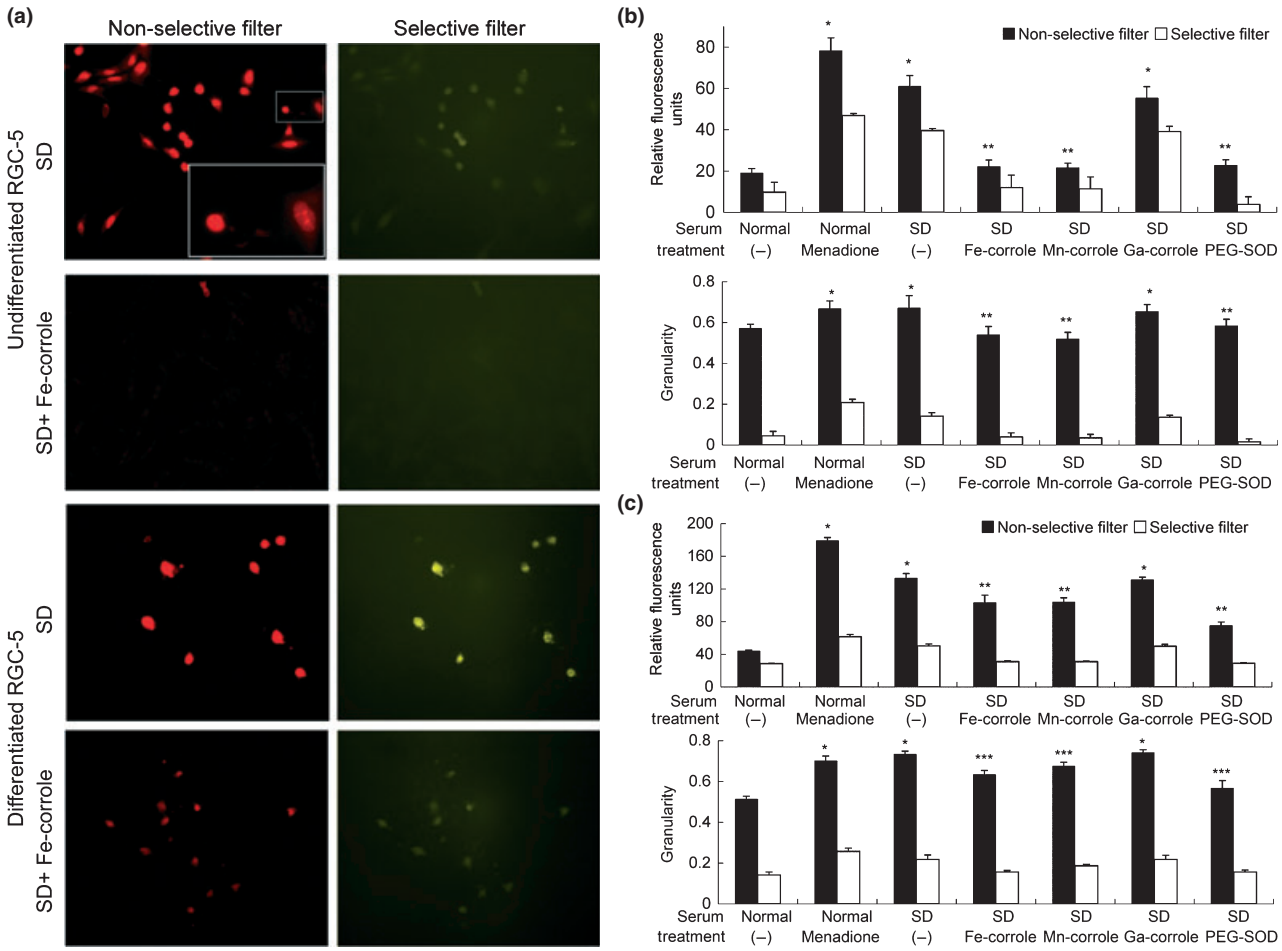

Fig. 5 (a) Undifferentiated and differentiated retinal ganglion cell (RGC)-5 cells were incubated with hydroethidine (HEt) to visualize superoxide. Serum-deprived RGC-5 cells were treated with metallocorroles at 100 nM or media control. Images were taken with either a non-selective filter set that detected oxidative products of HEt (pseudocolored red) or a filter set selective for 2-hydroxyethidium (2-OH-Et) (pseudocolored yellow). The inset shows magnified cells with high granularity (left) and low granularity (right). (b and c) Fluorescence intensity and granularity in undifferentiated (b) and differentiated (c) RGC-5 cells were calculated with ImageJ. Polyethylene glycol-conjugated superoxide dismutase (30 U/mL) was added in the absence of serum. Menadione (1 mM) was used in the presence of serum to induce mitochondrial superoxide production by redox cycling. Bars indicate results with filters non-selective (closed bars) and selective (open bars) for 2-OH-Et. *$p < 0.001$ compared with serum control condition. **$p < 0.001$ compared with serum-deprived condition. ***$p < 0.05$ compared with serum-deprived condition.

methamphetamine-induced neurotoxicity in rats (Imam *et al.* 2001). One potentially problematic chemical feature common to both metallocorroles and metalloporphyrins is that they may use ROS (e.g., hydrogen peroxide) for either catalyzing oxidation of other substrates (i.e., serving as pro-oxidants) or decomposing them (i.e., serve as anti-oxidants). One advantage of metallocorroles relative to metalloporphyrins is that their antioxidant property is more pronounced than their pro-oxidant capability.

Metallocorroles have also other properties that make them more useful for certain purposes than metalloporphyrins, such as the intense fluorescence of gallium corroles (Liu *et al.* 2008; Kowalska *et al.* 2009) that has been used for cellular and whole animal imaging (Agadjanian *et al.* 2009; Okun *et al.* 2009). Some reported metallocorroles have high water-solubility and amphiphilicity, which distinguishes them from most metalloporphyrins. In addition, Fe-, Mn-, and Ga-corroles form tightly bound non-covalent conjugates with variety of proteins, including serum albumins (Mahammed *et al.* 2004; Haber *et al.* 2004). In this study, coincubation with 1% BSA significantly decreased the toxicity of high concentrations of these metallocorroles on serum-deprived RGC-5 cells.

We studied both undifferentiated RGC-5 cells and RGC-5 cells differentiated with staurosporine. Undifferentiated RGC-5 cells are similar to neuronal precursor cells, dividing in culture and expressing an immature neuroglial morphology. Differentiated RGC-5 cells are post-mitotic, extend

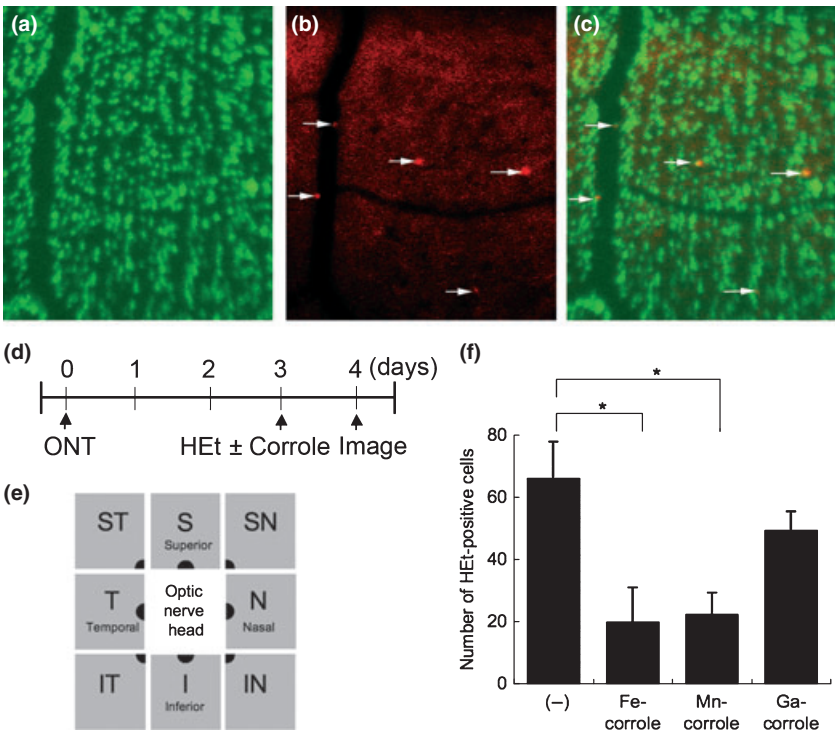

Fig. 6 (a–c) *In vivo* imaging confirmation that retinal ganglion cells express 2-hydroxyethidium (2-OH-Et) after optic nerve transection (ONT). (a) RGCs positive for 1,1′-dioctadecyl-3,3,3′,3′-tetramethylindotricarbocyanine iodide retrogradely transported from the superior colliculi were excited by the 788 nm laser. These cells are pseudocolored green. (b) 2-OH-Et-positive cells excited by the 488 nm laser after intravitreal administration of hydroethidine (HEt). These cells are pseudocolored red. (c) Merged image of (a) and (b). (d) Flowchart of experiments. (e) Schematic of topography of retinal imaging by confocal scanning laser ophthalmoscopy. To quantify the number of cells positive for 2-OH-Et, eight images were taken at each retinal octant adjacent to the optic nerve head. (f) The number of HEt-positive ganglion cell layer cells at 4 days after optic nerve transection in the presence or absence of Fe-, Mn-, and Ga-corroles. *$p < 0.05$.

neurites with characteristics of dendrites and axons, and therefore have the advantage of being similar to mature neurons. On the other hand, the drug used to differentiate RGC-5 cells, staurosporine, can also induce cytochrome *c* release (Lieven C. J. and Levin L. A., unpublished data) and low levels of baseline PI staining (Fig. 4), suggesting that some differentiated cells are undergoing apoptosis in our culture conditions. Because there are advantages and disadvantages for using both undifferentiated and differentiated cells, we studied the effects of metallocorroles in both models. Despite the differences in differentiation status, the superoxide scavenging and neuroprotective effects of Fe- and Mn-corroles were the same.

Our results indicate that the Fe- and Mn-corroles used in this study are able to decrease intracellular superoxide levels in neuronal precursor cells *in vitro* and retinal neurons *in vivo*. Serum deprivation was used in this study to induce neuronal cell death, via deprivation of molecules necessary for survival, including neurotrophic factors. One of the mechanisms by which neurotrophin deprivation causes apoptosis of neuronal cells is initiating production of intracellular ROS (Greenlund *et al.* 1995; Kirkland *et al.* 2007). We previously demonstrated that a critical molecular event underlying neuronal death after *in vitro* and *ex vivo* models of axonal injury is the generation of superoxide anion (Lieven *et al.* 2003, 2006; Nguyen *et al.* 2003). Real-time *in vivo* confocal imaging demonstrates that superoxide elevation precedes apoptosis in RGCs after optic nerve transection (Kanamori *et al.* in press) Using a similar *in vivo* imaging system in this study allowed us to measure intracellular superoxide within retinal neurons, based on the fluorescent product of superoxide with HEt. When HEt oxidation products are excited at 560 nm, both the superoxide-HEt product 2-OH-Et and the peroxide-HEt oxidation product Et can be visualized (Robinson *et al.* 2006). In our *in vivo* experiments, the 488 nm CSLO laser was used for excitation. We previously showed (Kanamori *et al.* in press) that the fluorescence detected with the CSLO with 488 nm excitation is mainly generated by the 2-OH-Et product (which is specific to superoxide), but there can also be fluorescence from Et, which is partially excited at that wavelength. To address this possibility, we previously correlated the *in vivo* imaging findings with histological examination of the same retinas using 395 nm excitation by epifluorescence microscopy (Kanamori *et al.* in press). These studies confirmed that the HEt-positivity detected *in vivo* arose from the superoxide product 2-OH-Et.

Using the CSLO for imaging of RGCs in living animals, we were able to show that intravitreal administration of Fe and Mn-corroles decreased retinal superoxide *in vivo*. This was supported by our finding that Fe- and Mn-corroles decrease superoxide levels in RGC-5 cells induced by serum deprivation. Together, these results suggest that Fe- and Mn-corroles may be useful as SOD mimetics for neuroprotective diseases associated with axonal injury.

Consistent with expectations, we showed that only Fe- and Mn-corroles, but not the redox-inactive Ga-corrole, were both neuroprotective and decomposed superoxide. We cannot exclude the possibility that catalytic decomposition of another ROS besides superoxide was the critical factor for

metallocorrole-mediated neuroprotection. Although we used a well-characterized model in which superoxide is known to both be generated and is necessary for RGC death, it could be that scavenging of HOONO (the product of superoxide and NO) contributed to increased neuronal survival *in vitro* at the same time that superoxide was being scavenged. Our previous work failed to find evidence for NO elevation in axotomized RGCs (Kanamori *et al.* in press), but perhaps a basal level of NO could combine with elevated superoxide to induce cell death. Measurements of ROS scavenging (Table 1) reveals that Mn-corrole is a significantly poorer HOONO scavenger than Fe-corrole, yet our assays demonstrated that these metallocorroles were almost equally neuroprotective of serum-deprived neuronal cells. Nonetheless, without more specific scavengers or a method for imaging HOONO with high specificity, the possibility that decomposition of HOONO is responsible for neuroprotection in this paradigm cannot be completely excluded.

There are few studies of metallocorroles as cytoprotectants *in vitro* or *in vivo*. Haber *et al.* (2008) compared oral Fe-, Mn-, and Ga-corroles in a mouse model of atherosclerosis. They found that Fe-corrole dramatically prevented the development of atherosclerotic lesions and that Mn-corrole moderately reduced the size of lesion. Ga-corrole had no effect on the lesions despite reducing blood cholesterol levels (Fe: 40%, Mn: 26%, Ga: 20%). Kupershmidt *et al.* (2010) showed that Fe- and Mn-corroles increased survival of human neuroblastoma and mouse motor neuron-neuroblastoma fusion cells when treated with 3-morpholinosydnonimine, which generates HOONO, or with 6-hydroxydopamine, which generates a variety of ROS. Our findings indicate that Fe- and Mn-corroles could be candidate therapeutic agents for diseases associated with axonal injury where superoxide may be a critical factor. Such diseases include optic neuropathies such as glaucoma, where treatment does not always prevent progression, and non-arteritic anterior ischemic optic neuropathy, where there is no effective treatment. The use of specific metallocorroles may make possible the treatment of such diseases and potentially other superoxide-associated conditions, such as physiological aging.

Acknowledgements

Canadian Institutes for Health Research, Canadian Foundation for Innovation, Canadian Research Chairs program, Fonds de recherche en ophtalmologie de l'Université de Montréal, National Institutes of Health. Work at the Technion was supported by the Herbert Irving Cancer and Atherosclerosis Research Fund and the Israel Science Foundation.

Author disclosure statement

No competing financial interests exist.

References

Agadjanian H., Ma J., Rentsendorj A., Valluripalli V., Youn Hwang J., Mahammed A., Farkas D. L., Gray H. B., Gross Z. and Medina-Kauwe L. K. (2009) Tumor detection and elimination by a targeted gallium corrole. *Proc. Nat. Acad. Sci.* **106**, 6100–6105.

Agadjanian H., Weaver J. J., Mahammed A. *et al.* (2006) Specific delivery of corroles to cells via noncovalent conjugates with viral proteins. *Pharm. Res.* **23**, 367–377.

Aviv I. and Gross Z. (2007) Corrole-based applications. *Chem. Commun. (Camb.)* 1987–1999.

Aviv-Harel I. and Gross Z. (2009) Aura of corroles. *Chemistry* **15**, 8382–8394.

Batinic-Haberle I., Benov L., Spasojevic I. and Fridovich I. (1998) The ortho effect makes manganese(III) meso-tetrakis(N-methylpyridinium-2-yl)porphyrin a powerful and potentially useful superoxide dismutase mimic. *J. Biol. Chem.* **273**, 24521–24528.

Berkowitz B. A., Lukaszew R. A., Mullins C. M. and Penn J. S. (1998) Impaired hyaloidal circulation function and uncoordinated ocular growth patterns in experimental retinopathy of prematurity. *Invest. Ophthalmol. Vis. Sci.* **39**, 391–396.

Crow J. P. (1999) Manganese and iron porphyrins catalyze peroxynitrite decomposition and simultaneously increase nitration and oxidant yield: implications for their use as peroxynitrite scavengers in vivo. *Arch. Biochem. Biophys.* **371**, 41–52.

Cuzzocrea S., Riley D. P., Caputi A. P. and Salvemini D. (2001) Antioxidant therapy: a new pharmacological approach in shock, inflammation, and ischemia/reperfusion injury. *Pharmacol. Rev.* **53**, 135–159.

Day B. J., Fridovich I. and Crapo J. D. (1997) Manganic porphyrins possess catalase activity and protect endothelial cells against hydrogen peroxide-mediated injury. *Arch. Biochem. Biophys.* **347**, 256–262.

Eckshtain M., Zilbermann I., Mahammed A., Saltsman I., Okun Z., Maimon E., Cohen H., Meyerstein D. and Gross Z. (2009) Superoxide dismutase activity of corrole metal complexes. *Dalton Trans.* 7879–7882.

Frassetto L. J., Schlieve C. R., Lieven C. J., Utter A. A., Jones M. V., Agarwal N. and Levin L. A. (2006) Kinase-dependent differentiation of a retinal ganglion cell precursor. *Invest. Ophthalmol. Vis. Sci.* **47**, 427–438.

Greenlund L. J., Deckwerth T. L. and Johnson E. M. (1995) Superoxide dismutase delays neuronal apoptosis: a role for reactive oxygen species in programmed neuronal death. *Neuron* **14**, 303–315.

Gross Z. and Galili N. (1999) N-Substituted Corroles: A Novel Class of Chiral Ligands. *Angew Chem. Int. Ed. Engl.* **38**, 2366–2369.

Gryko D. T. (2002) Recent advances in the synthesis of corroles and core-modified corroles. *Eur. J. Org. Chem.* **2002**, 1735–1743.

Haber A., Agadjanian H., Medina-Kauwe L. K. and Gross Z. (2008) Corroles that bind with high affinity to both apo and holo transferrin. *J. Inorg. Biochem.* **102**, 446–457.

Haber A., Mahammed A., Fuhrman B., Volkova N., Coleman R., Hayek T., Aviram M. and Gross Z. (2008) Amphiphilic/Bipolar metallocorroles that catalyze the decomposition of reactive oxygen and nitrogen species, rescue lipoproteins from oxidative damage, and attenuate atherosclerosis in mice. *Angew Chem. Int. Ed. Engl.* **47**, 7896–7900.

Imam S. Z., el-Yazal J., Newport G. D., Itzhak Y., Cadet J. L., Slikker W. Jr and Ali S. F. (2001) Methamphetamine-induced dopaminergic neurotoxicity: role of peroxynitrite and neuroprotective role of antioxidants and peroxynitrite decomposition catalysts. *Ann. NY Acad. Sci.* **939**, 366–380.

Kanamori A., Catrinescu M. M., Traistaru M., Beaubien R. and Levin L. A. (2010) In vivo imaging of retinal ganglion cell axons within the nerve fiber layer. *Invest. Ophthalmol. Vis. Sci.* **51**, 2011–2018.

Kanamori A., Catrinescu M., Kanamori N., Mears K. A., Beaubien R. and Levin L. A. (in press) Superoxide is an associated signal for apoptosis in axonal injury. *Brain*, in press.

Kirkland R. A., Saavedra G. M. and Franklin J. L. (2007) Rapid activation of antioxidant defenses by nerve growth factor suppresses reactive oxygen species during neuronal apoptosis: evidence for a role in cytochrome c redistribution. *J. Neurosci.* **27**, 11315–11326.

Kowalska D., Liu X., Tripathy U., Mahammed A., Gross Z., Hirayama S. and Steer R. P. (2009) Ground- and excited-state dynamics of aluminum and gallium corroles. *Inorg. Chem.* **48**, 2670–2676.

Kupershmidt L., Okun Z., Amit T., Mandel S., Saltsman I., Mahammed A., Bar-Am O., Gross Z. and Youdim M. B. (2010) Metallocorroles as cytoprotective agents against oxidative and nitrative stress in cellular models of neurodegeneration. *J. Neurochem.* **113**, 363–372.

Lieven C. J., Vrabec J. P. and Levin L. A. (2003) The effects of oxidative stress on mitochondrial transmembrane potential in retinal ganglion cells. *Antioxid. Redox Signal.* **5**, 641–646.

Lieven C. J., Schlieve C. R., Hoegger M. J. and Levin L. A. (2006) Retinal ganglion cell axotomy induces an increase in intracellular superoxide anion. *Invest. Ophthalmol. Vis. Sci.* **47**, 1477–1485.

Liu X., Mahammed A., Tripathy U., Gross Z. and Steer R. P. (2008) Photophysics of Soret-excited tetrapyrroles in solution. III. Porphyrin analogues: aluminum and gallium corroles. *Chem. Phys. Lett.* **459**, 113–118.

Mackensen G. B., Patel M., Sheng H. *et al.* (2001) Neuroprotection from delayed postischemic administration of a metalloporphyrin catalytic antioxidant. *J. Neurosci.* **21**, 4582–4592.

Mahammed A. and Gross Z. (2005) Albumin-conjugated corrole metal complexes: extremely simple yet very efficient biomimetic oxidation systems. *J. Am. Chem. Soc.* **127**, 2883–2887.

Mahammed A. and Gross Z. (2006) Iron and manganese corroles are potent catalysts for the decomposition of peroxynitrite. *Angew Chem. Int. Ed. Engl.* **45**, 6544–6547.

Mahammed A., Gray H. B., Weaver J. J., Sorasaenee K. and Gross Z. (2004) Amphiphilic corroles bind tightly to human serum albumin. *Bioconjug. Chem.* **15**, 738–746.

Misko T. P., Highkin M. K., Veenhuizen A. W., Manning P. T., Stern M. K., Currie M. G. and Salvemini D. (1998) Characterization of the cytoprotective action of peroxynitrite decomposition catalysts. *J. Biol. Chem.* **273**, 15646–15653.

Nguyen S. M., Alexejun C. N. and Levin L. A. (2003) Amplification of a reactive oxygen species signal in axotomized retinal ganglion cells. *Antioxid. Redox Signal.* **5**, 629–634.

Okun Z., Kupershmidt L., Amit T., Mandel S., Bar-Am O., Youdim M. B. and Gross Z. (2009) Manganese corroles prevent intracellular nitration and subsequent death of insulin-producing cells. *ACS Chem. Biol.* **4**, 910–914.

Pacher P., Beckman J. S. and Liaudet L. (2007) Nitric oxide and peroxynitrite in health and disease. *Physiol. Rev.* **87**, 315–424.

Robinson K. M., Janes M. S., Pehar M., Monette J. S., Ross M. F., Hagen T. M., Murphy M. P. and Beckman J. S. (2006) Selective fluorescent imaging of superoxide in vivo using ethidium-based probes. *Proc. Natl Acad. Sci. USA* **103**, 15038–15043.

Saltsman I., Mahammed A., Goldberg I., Tkachenko E., Botoshansky M. and Gross Z. (2002) Selective substitution of corroles: nitration, hydroformylation, and chlorosulfonation. *J. Am. Chem. Soc.* **124**, 7411–7420.

Salvemini D., Wang Z. Q., Zweier J. L. *et al.* (1999) A nonpeptidyl mimic of superoxide dismutase with therapeutic activity in rats. *Science* **286**, 304–306.

Schlieve C. R., Lieven C. J. and Levin L. A. (2006) Biochemical activity of reactive oxygen species scavengers do not predict retinal ganglion cell survival. *Invest. Ophthalmol. Vis. Sci.* **47**, 3878–3886.

Sheng H., Enghild J. J., Bowler R. *et al.* (2002) Effects of metalloporphyrin catalytic antioxidants in experimental brain ischemia. *Free Radic. Biol. Med.* **33**, 947–961.

Torreilles F., Salman-Tabcheh S., Guerin M. and Torreilles J. (1999) Neurodegenerative disorders: the role of peroxynitrite. *Brain Res. Brain Res. Rev.* **30**, 153–163.

Zhao H., Kalivendi S., Zhang H., Joseph J., Nithipatikom K., Vasquez-Vivar J. and Kalyanaraman B. (2003) Superoxide reacts with hydroethidine but forms a fluorescent product that is distinctly different from ethidium: potential implications in intracellular fluorescence detection of superoxide. *Free Radic. Biol. Med.* **34**, 1359–1368.

